ICA 2016 BUENOS AIRES
Buenos Aires – 5 to 9 September 2016
Acoustics for the 21st Century...

PROCEEDINGS of the 22nd International Congress on Acoustics

Acoustic Array System: Near-field Acoustic Holography and Vibro-Acoustic Field Reconstruction: Paper ICA2016-813

Separation of track contribution to pass-by noise by near-field array techniques

Elias Zea[(a)], **Luca Manzari**[(a)], **Ines Lopez Arteaga**[(a,b)], **Giacomo Squicciarini**[(c)], **David Thompson**[(c)]

[(a)]KTH Royal Institute of Technology, The Marcus Wallenberg Laboratory for Sound and Vibration Research, Sweden, zea@kth.se
[(b)]Eindhoven University of Technology, Department of Mechanical Engineering, The Netherlands, I.Lopez@tue.nl
[(c)]University of Southampton, Institute of Sound and Vibration Research, UK, djt@isvr.soton.ac.uk

Abstract

A technique to separate the track noise contribution is proposed based on identifying and extracting the track signature from the pass-by noise information measured with a microphone array relatively close to the track. Separation of the contributions of the vehicle and the track in the pass-by noise spectra is a challenging task, which is currently addressed by a combination of direct and indirect measurements and model predictions. Due to the uncertainties in the separation of the track contribution, whether a vehicle will comply with regulations during certification tests is still very much track dependent. Therefore, accurate means to identify the track contribution to the pass-by noise are needed. In this paper we propose to make use of the fact that in a wide frequency range the track is a distributed source that radiates plane waves at a given angle with respect to the track. By measuring the sound field close to the track with a microphone array, the wavenumber spectrum of the radiated sound can be determined. For the track contribution this wavenumber spectrum is tonal and therefore sparse. We make use of this property to design filters that extract the track contribution to the total pass-by noise. This is illustrated with simulations and experiments.

Keywords: railway, track, noise, NAH, separation

Separation of track contribution to pass-by noise by near-field array techniques

1 Introduction

The characterization of the dominant noise sources during a train pass-by provides a means for counteracting the problem of railway noise generation and annoyance. For a running train with velocities up to 300 km/h [1], the prevailing noise source is that due to the interaction of the vehicle wheels and the track, also known as rolling noise. To further distinguish (or separate) the wheel noise from the track noise has been a problem of interest in the past decades.

Work towards this direction began with the TWINS model [2], which offers accurate means to predict the sound power radiated by the separate noise sources during a train pass-by. TWINS has been experimentally validated [3, 4], and it requires knowledge of the wheel and track roughnesses and track decay rate as prior information. An approach other than TWINS is the transfer function method [5], which provides an indirect estimation of the transfer functions of the vehicle and the track. The method requires an accelerometer on one of the tracks, and a microphone located 1.2 m above the ground and 7.5 m from the mid-point between the tracks.

Another approach is to use microphone arrays. On the one hand, beamforming has been employed in a number of occasions [6, 7, 8], yet with no success because the separated sound fields give more prominence to the wheel than to the track contribution. The weakness of beamforming in this scenario is the assumption that the acoustic sources are uncorrelated, thus a spatially extended source such as the track is hardly detectable –even if the antenna is steered towards the radiation angle of the track. On the other hand, the so-called SWEAM method has been proposed in [9], which is an inverse method that computes a least-squares estimate of the measured pressure field that best approximates the field radiated by the rail.

The approach followed in the present paper is to perform near-field microphone array measurements during the pass-by, and filter the track contribution in the wavenumber domain by means of spatial Fourier transforms. The filter design is based on the spatial distribution of the rolling noise sources and knowledge of the structural response of the track.

2 Theory

This section provides an overview of the theory that covers the presented method, hereafter called wave signature extraction (WSE). The idea is to extract the track signature from the wavenumber spectrum of the pass-by measured by a line microphone array. The block diagram below shows the steps performed in the method.

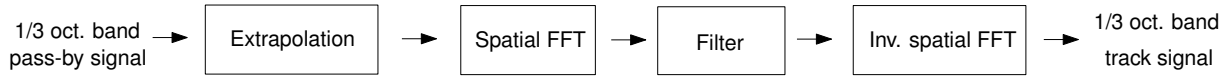

Figure 1: **Block diagram of the wave signature extraction method.**

2.1 Mathematical basis

The WSE is based on two mathematical concepts: signal sparsity and signal power. Signal sparsity is related to the spatial distribution of the sources: a train wheel is spatially compact and radiates omnidirectionally, while a railway track is spatially extended and radiates plane waves at a certain angle with respect to the track [7]. In the wavenumber domain, this is equivalent to a broadband spectrum for the wheel and a narrowband spectrum for the track.

On the other hand, a narrowband filter is purposeful when the narrowband content is above the noise floor. Therefore, in the context of rolling noise separation, filtering is expected to perform well if the track contribution (narrowband) has a greater signal power than the wheel contribution ("noise floor"). According to TWINS simulations, this is true for sound power within the frequency range of 500-1600 Hz (depending on the pad stiffness) [4], thus this fact is exploited in the WSE method.

2.2 Sound field extrapolation

In order to refine the wavenumber spectra, data extrapolation is applied in the spatial domain prior to spatial Fourier transformation, per frequency component. The technique adopted is second-order linear-predictive border padding [10], which fits an auto-regressive model to the measured sound field so as to predict the extrapolated samples.

2.3 Filter design

The choice of filter in the wavenumber domain is a low-pass function since the track signal is narrowband and has a smaller bandwidth than the wheel signal. This fact comes from the spatial distribution of the sources (see Section 2.1). The mathematical formulation follows:

$$H(k_x) = \frac{1}{\sqrt{\left(1+\mathrm{j}\frac{k_x}{k_{co}}\right)\left(1-\mathrm{j}\frac{k_x}{k_{co}}\right)}^{n}}, \tag{1}$$

where k_x is the wavenumber along the x-axis, j is the imaginary unit, k_{co} is the cut-off wavenumber of the filter, and $n \geq 1$ is the filter order. In essence, this filter has one pole, and is zero-phase since it only alters the magnitude of the input signal: $-3n$ dB at cut-off point, with decay rate of $-20n$ dB per wavenumber decade.

In order to choose the filter cut-off and order, knowledge of the structural response of the track can be used. This can be obtained from a validated track model (e.g. a Timoshenko beam), or from impact testing on the track prior to the train pass-by. The argument to support this approach is that the acceleration (or mobility) spectra have the same bending wavenumbers as the pressure spectra.

3 Numerical simulations

A steady-state model of the wheel and the track is used to investigate the method with synthetic data. The acoustic fields have a time-harmonic dependence $e^{\mathrm{j}\omega t}$.

3.1 Sound radiation model

The geometry of the model is illustrated in Figure 2. The sound radiation of the rail is modelled with the equivalent source method (ESM) as performed in [7]. The velocity of the track corresponds to that of a periodically supported Timoshenko beam, and two pad stiffnesses are considered: stiff ($4.1 \cdot 10^8$ N/m) and soft (10^8 N/m). The remaining track parameters are taken from [7]. The wheel radiation is modelled as a monopole source [2], located 35 cm above the rail ESM. The rail and wheel pressure fields are summed, and complex Gaussian noise is added such that the signal-to-noise ratio (SNR) is 15 dB. The line microphone array has 60 transducers inter-spaced by 8 cm, and it is positioned 50 cm away from the rail. For this particular microphone spacing, the highest alias-free frequency corresponds to about 2.1 kHz.

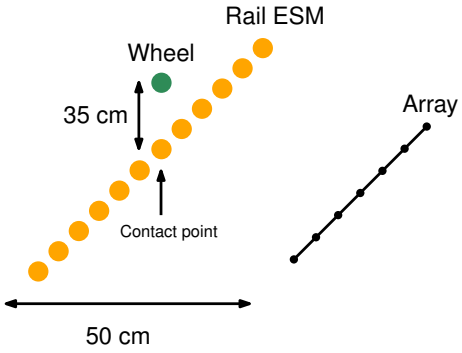

Figure 2: **Geometrical sketch of the numerical simulations.**

In order to study a scenario closer to a train pass-by, we make use of relative sound power of rail and wheel contributions based on TWINS data (see Figure 3). To do this, we define a rail-to-wheel ratio (RWR) per frequency component as:

$$\mathrm{RWR} = 20 \log_{10} \frac{\|\mathbf{p}_{\mathrm{rail}}\|_2}{\|\mathbf{p}_{\mathrm{wheel}}\|_2}, \tag{2}$$

where $\mathbf{p}_{\mathrm{rail}}$ and $\mathbf{p}_{\mathrm{wheel}}$ are the pressure fields of the rail and wheel signals measured at the line array. It is equivalent to the signal power ratio between rail and wheel in decibels. On the other hand, the wheel pressure at the i-th microphone follows by definition: $(\mathbf{p}_{\mathrm{wheel}})_i = S \frac{\mathrm{e}^{-\mathrm{j}kr_i}}{r_i}$, where S is the monopole strength, k is the acoustic wavenumber, and r_i is the distance from the monopole to the microphone position. By defining $\mathbf{p}^0_{\mathrm{wheel}}$ as a unit-strength monopole, it follows that $\|\mathbf{p}_{\mathrm{wheel}}\|_2 = S\|\mathbf{p}^0_{\mathrm{wheel}}\|_2$. Hence substituting this relationship into Eq. 2 yields

$$S = \frac{\|\mathbf{p}_{\mathrm{rail}}\|_2}{\|\mathbf{p}^0_{\mathrm{wheel}}\|_2} 10^{-\frac{\mathrm{RWR}}{20}}. \tag{3}$$

The wheel monopole strengths can be computed by means of equating the signal power ratios (RWR) to rail-to-wheel sound power differences from TWINS. Then the total "measured" field equals the rail's ESM field plus the monopole field and the added complex noise.

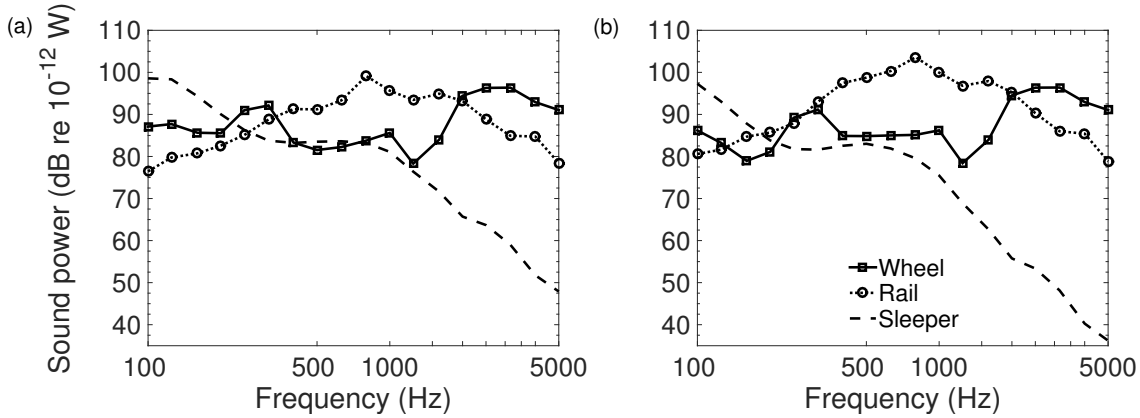

Figure 3: **Sound power in 1/3 octave frequency bands of wheel, rail and sleeper noise contributions, based on TWINS data, for a track with (a) stiff and (b) soft pads.**

3.2 Filtering

The filtering procedure in the wavenumber domain is illustrated in Figure 4, showing the spectra of the relevant fields, along with the filter response and the filtered (recovered) signal. It can be seen for this frequency that the rail signature is approximately found within the wavenumber bandwidth $(-5,5)$ rad/m, whereas the wheel covers a bandwidth of about $(-20,20)$ rad/m. It can also be appreciated how the added noise is filtered from the measured field spectrum.

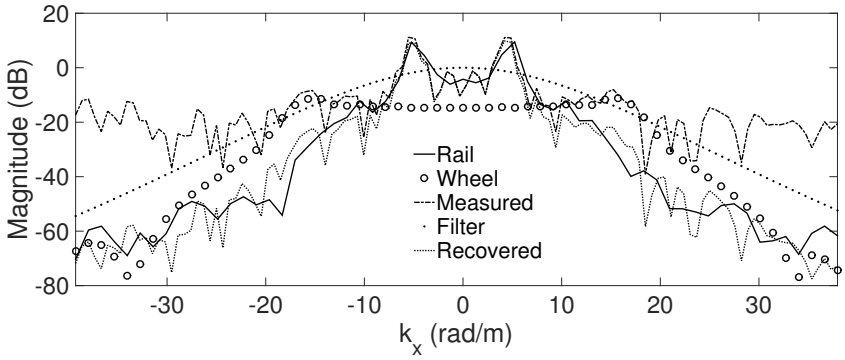

Figure 4: **Wavenumber spectra of the rail, wheel and (total) measured fields, as well as the filter response and the recovered rail signal at 1000 Hz and for a track with soft pads.**

3.3 Recovery errors

In order to quantify the accuracy of the method, we make use of a recovery error metric

$$\varepsilon = 20\log_{10}\frac{\|\mathbf{p}_{\text{rec}} - \mathbf{p}_{\text{ref}}\|_2}{\|\mathbf{p}_{\text{ref}}\|_2}, \tag{4}$$

where $\mathbf{p}_{\text{rec}}$ and $\mathbf{p}_{\text{ref}}$ are the recovered and reference track pressure fields respectively.

The recovery errors versus frequency for both pad stiffnesses are shown in Figure 5. The filter cut-off wavenumbers are chosen from knowledge of the mobility wavenumber spectrum of the Timoshenko beam. The filter order is 10 and is chosen from empirical observations. No apparent differences in recovery errors, except at 500 Hz, are found with respect to the pad stiffness.

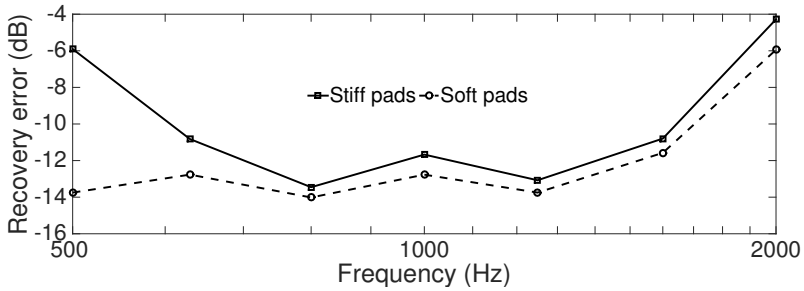

Figure 5: **Recovery errors in dB as a function of frequency for stiff and soft pads.**

Furthermore, the recovered and reference track pressure fields are shown in Figures 6 and 7 for both stiff and soft pads respectively, and at 500, 1000 and 2000 Hz. The "measured" fields are also shown. Overall, the recovered sound fields resemble the reference sound fields, and the accuracy of the method is linked to the RWR values: more accurate as the RWR increases.

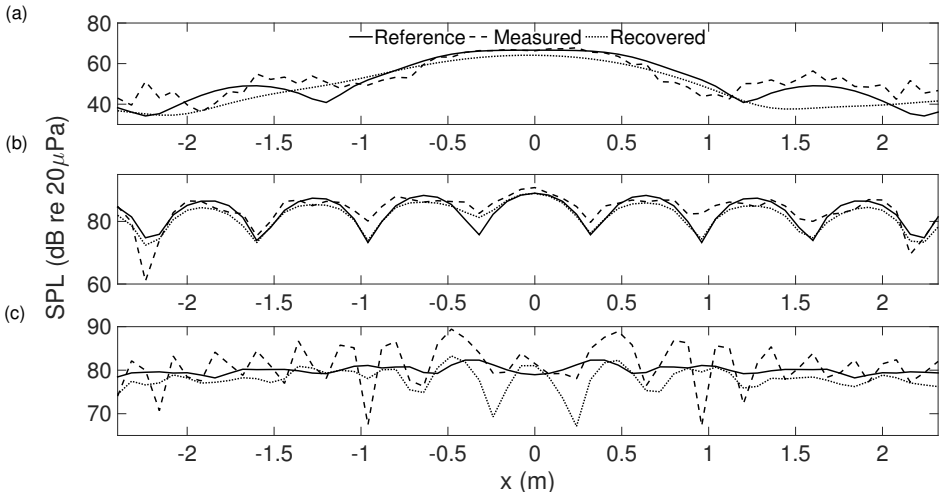

Figure 6: **Reference, measured and recovered sound pressure levels for a track with stiff pads, at (a) 500, (b) 1000 and (c) 2000 Hz.**

The following section includes a few field tests, prior to the pass-by measurements, that have been performed to explore possible means of extracting the rail signature, as well as evaluate the influence of the vehicle load in such signature.

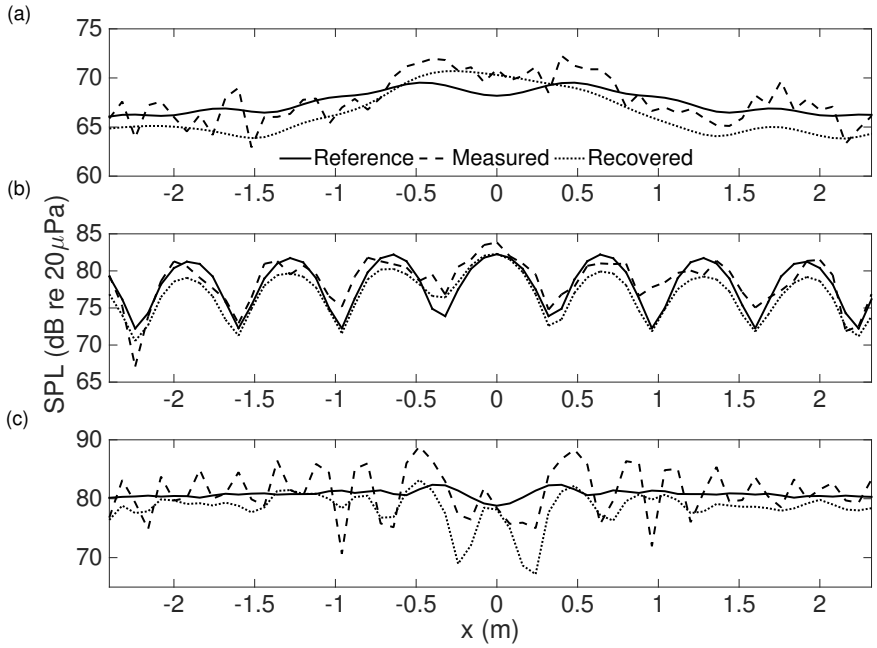

Figure 7: **Reference, measured and recovered sound pressure levels for a track with soft pads, at (a) 500, (b) 1000 and (c) 2000 Hz.**

4 Field measurements

The measurements are in static conditions following an impact testing protocol, and were done in a test track section at Bombardier Transportation Västerås (Sweden), in October 2015 and March 2016. The track has no pads and the sleepers are made of concrete. Photographs of the setup are shown in Figure 8. A total of 60 microphone positions inter-spaced by 5 cm are measured by means of shifting a 20 microphone line array, and a total of 28 acceleration points inter-spaced by 8 cm are measured. Three main results are shown here: (i) comparison of dispersion curves obtained from accelerometers and from microphones, (ii) influence of spatial extrapolation on the track signature, and (iii) influence of the vehicle on the dispersion curves.

4.1 Acceleration and pressure dispersion

For the sake of showing that the bending wavenumbers of the track are independent of the method used to measure them, the dispersion plot for both pressure and acceleration data is shown in Figure 9. Minor differences can be seen and are attributed to the smaller aperture (greater leakage) in the acceleration data than that of the microphone array. This allows for filter design, specially the cut-off wavenumber, based on the bending wavenumbers of the track obtained from the acceleration dispersion curve prior to the pass-by.

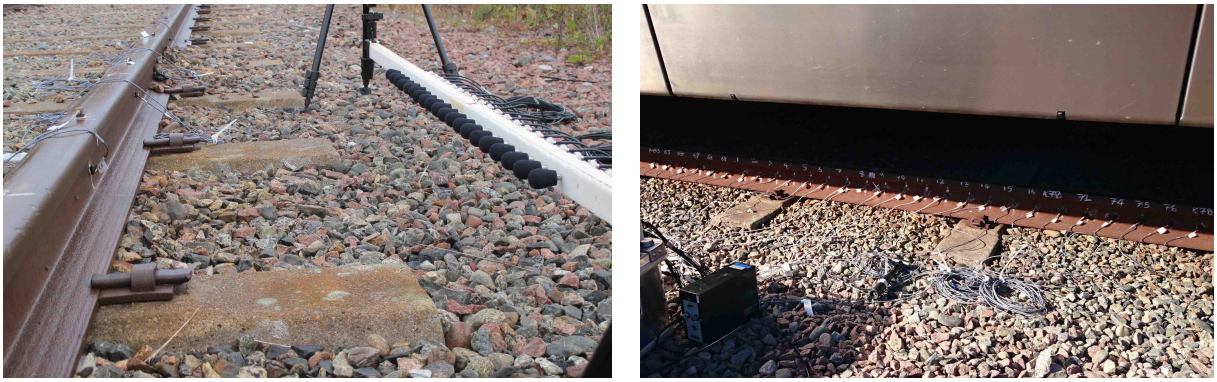

(a) (b)

Figure 8: **Photographs of the experimental setup: (a) microphone array measurement on empty track, and (b) acceleration measurement with train X2000 on the track.**

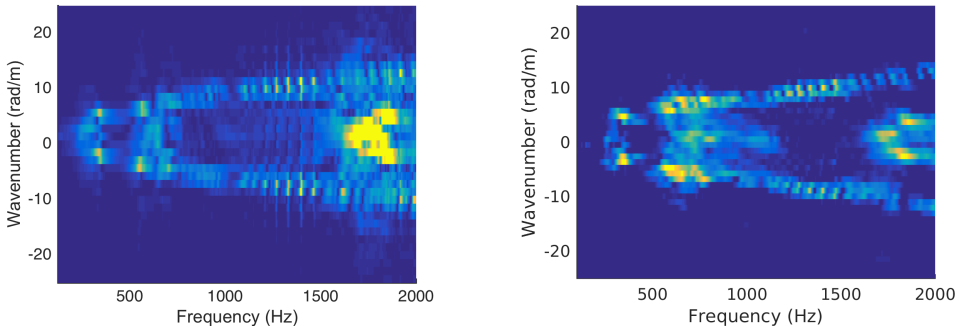

Figure 9: **Dispersion plot obtained from (a) acceleration and (b) pressure data**.

4.2 Influence of extrapolation

In order to illustrate the significance of sound field extrapolation, Figure 10 shows the dispersion curve obtained from a measurement with 60 microphone positions, and that obtained from an extrapolated measurement to 120 microphone positions. It is possible then to see how the signature can be sharpened by means of extrapolating spatial data. This is expected to improve the separation during the pass-by measurements since it lessens the leakage in wavenumber domain due to windowing prior to Fourier transformation.

4.3 Influence of vehicle load

The presence of the train is expected to increase the mass of the whole system, which might introduce a frequency shift in the dispersion curve. Figure 11 shows the dispersion plots obtained from acceleration data, without and with the train on the track, and the difference in dB

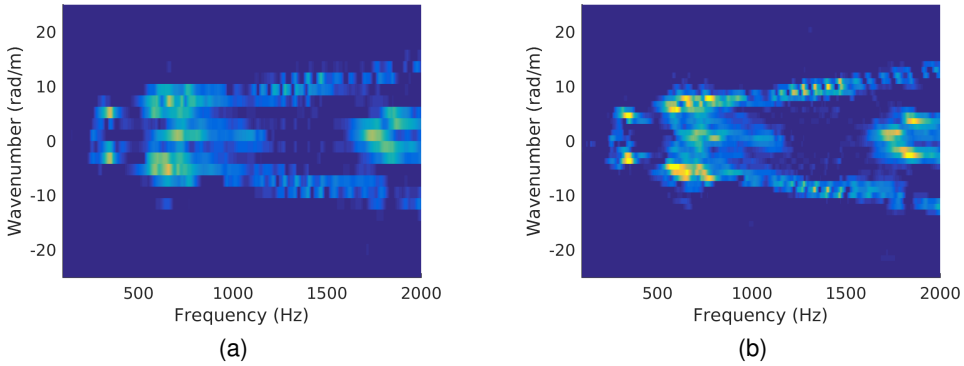

Figure 10: **Dispersion plot obtained from (a) original and (b) extrapolated microphone array data.**

of the two plots. These results indicate that the dispersion plot varies between 1% and 5% in the presence of the train, most noticeably around 1.8 kHz; otherwise not significantly varying.

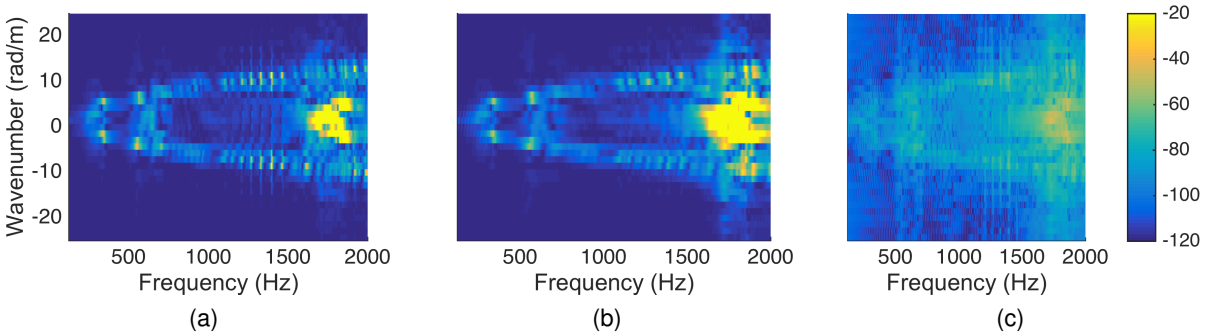

Figure 11: **Dispersion plot obtained with acceleration data (a) without and (b) with the train on the track. (c) Difference in dB (color bar) between (a) and (b).**

5 Conclusions

We introduce a new technique for the purpose of separating the track contribution from railway vehicle pass-by noise, by means of microphone array measurements in the near-field of the railway track. The separation is performed in the wavenumber domain with a low-pass filter function that is designed from knowledge of the structural response of the track. The method is numerically investigated with a sound radiation model, and, overall, the results indicate that the method is promising. Field experiments have been performed under static conditions, to explore methods to measure the rail signature and the influence of the vehicle load on this.

Acknowledgements

This work is part of the project Roll2Rail, which is financially supported by the European Union's Horizon 2020, gran agreement No.: 636032. Acknowledgements are given to Bombardier Transportation for providing the test track section and assisting in planning, and to Leping Feng for the support during field tests.

References

[1] Gautier, P.; Poisson, F.; Létourneaux, F. High speed train external noise: recent results in the TGV case. Proceedings of the 19th International Congress on Acoustics, Madrid, Spain, September 2-7, 2007. In CD-ROM.

[2] Thompson, D. Railway noise and vibration, Elsevier, Oxford (UK), 1st edition, 2009.

[3] Thompson, D.; Hemsworth, B.; Vincent, N. Experimental validation of the TWINS prediction program, part 1: description of the model and method. Journal of Sound and Vibration, 193 (1), 1996, pp 123-135.

[4] Thompson, D.; Fodiman, P.; Mahé, H. Experimental validation of the TWINS prediction program, part 2: results. Journal of Sound and Vibration, 193 (1), 1996, pp 137-147.

[5] Janssens, M.; Dittrich, M.; de Beer, F.; Jones, C. Railway noise measurement method for pass-by noise, total effective roughness, transfer functions and track spatial decay. Journal of Sound and Vibration, 293 (3-5), 2006, pp. 1007-1028.

[6] Kitagawa, T.; Thompson, D. Comparison of wheel/rail noise radiation on Japanese railways using the TWINS model and microphone array measurements. Journal of Sound and Vibration, 293 (3-5), 2006, pp 496-509.

[7] Kitagawa, T.; Thompson, D. The horizontal directivity of noise radiated by a rail and implications for the use of microphone arrays. Journal of Sound and Vibration, 329 (2), 2010, pp 202-220.

[8] Le Courtois, F.; Thomas, J.-H.; Poisson, F.; Pascal, J.-C. Identification of the rail radiation using beamforming and a 2 D array. Proceedings of the Acoustics 2012 Nantes Conference, France, April 23-27, 2012, pp 3745-3750.

[9] Faure, B.; Chiello, O.; Pallas, M.-A.; Servière, C. Characterisation of the acoustic field radiated by a rail with a microphone array: The SWEAM method. Journal of Sound and Vibration, 346, 2015, pp 165-190.

[10] Scholte, R.; Lopez Arteaga, I.; Roozen, B.; Nijmeijer, H. Truncated aperture extrapolation for Fourier-based near-field acoustic holography by means of border-padding. The Journal of the Acoustical Society of America, 125 (6), 2009, pp 3844-3854.